DMD Fast Forward. Published on May 26, 2011 as doi:10.1124/dmd.111.039529

DMD # 39529

In vitro metabolism of the mycotoxin enniatin B in different species and CYP P450 enzyme phenotyping by chemical inhibitors

Christiane K. Fæste, Lada Ivanova, Silvio Uhlig

Norwegian Veterinary Institute, P.O Box 750 Sentrum, N-0106 Oslo, Norway

DMD # 39529

Running Title:

Enniatin B *in vitro* metabolism and CYP-enzyme phenotyping

Address correspondence to:

Christiane Kruse Fæste, PhD

Section of Chemistry and Toxicology, Norwegian Veterinary Institute, P.O Box 750 Sentrum, N-0106 Oslo, Norway.

Tel.: +47 23216221; fax: +47 23216201

E-mail: christiane.faste@vetinst.no

Number of Text Pages: 21

Number of Tables: 3

Number of Figures: 6

Number of References: 40

Number of words in the Abstract: 245

Number of words in the Introduction: 742

Number of words in the Discussion: 1480

List of non-standard abbreviations:

Enniatin B: EnnB

Metabolite 1: M1

Abstract

Enniatins are cyclic hexapeptidic mycotoxins produced by fungi growing on field grains especially in wet climates. They show considerable resistance to food and feed processing technologies and might cause intoxication of humans and animals. Enniatins are also under exploration as anti-cancer drugs. The observed difference of *in vitro* and *in vivo* toxicities suggests low absorption or fast elimination of the enniatins after oral uptake. In the present study, *in vitr*o metabolism studies of enniatin B were performed using rat, dog, and human liver microsomes under conditions of linear kinetics to estimate the respective elimination rates. Furthermore, cytochrome P450 reaction phenotyping with chemical inhibitors selective for human enzymes was carried out. Twelve metabolites were separated and characterized by multiple high-performance liquid chromatographic/mass spectrometric analyses as products of oxidation and demethylation reactions. Biotransformation rates and metabolite patterns varied considerably in the three species. The intrinsic clearances determined in assays with rat, dog and human liver microsomes were 1.16 l/(h*kg), 8.23 l/(h*kg), and 1.13 l/(h*kg), respectively. The predicted enniatin B *in vivo* blood clearances were 1.57 l/(h*kg) in rats, 1.67l/(h*kg) in dogs and 0.63 l/(h*kg) in humans. CYP3A4 was important for enniatin B metabolism in human microsomes as shown by 80 % inhibition and impaired metabolite formation in the presence of troleandomycin. CYP1A2 and CYP 2C19 were additionally involved. Preliminary results showed that CYP3A and CYP1A might also be relevant in rats and dogs. The extensive hepatic metabolism could explain the reduced *in vivo* potential of enniatin B.

DMD Fast Forward. Published on May 26, 2011 as DOI: 10.1124/dmd.111.039529
This article has not been copyedited and formatted. The final version may differ from this version.

Introduction

Enniatins are secondary fungal metabolites that are mainly produced by *Fusarium* strains, which belong to the most common cereal contaminants (Uhlig et al., 2007; Jestoi, 2008). Grains in Northern Europe were contaminated with high levels of enniatins in recent years adding up to maximum concentrations of 7.7 mg/kg and 24.8 mg/kg in Norwegian and Finnish wheat, respectively (Uhlig et al., 2007). In Mediterranean countries, wheat and sorghum containing up to 493 mg/kg and 696 mg/kg enniatins, respectively, were observed (Queslati et al., 2011; Mahnine et al., 2011). Enniatin B (EnnB), the most prevalent among the 28 homologues identified (Firáková et al., 2007), is a cyclic hexadepsipeptide consisting of three D-2-hydroxyisovaleric acid (Hiv) residues linked alternatively to three *N*-methyl-L-valines (N-Me-Val) resulting in a 18-membered $(\text{N-Me-Val-Hiv})_3$ - molecule with the molecular formula and weight $C_{36}H_{63}N_3O_9$ and 639.83 g/mol (Figure 1) (Blais et al, 1992).

EnnB is considerable resistant to heat (melting point: 173-175 °C) (Altomare et al. 1995), acids and digestion and has been shown to propagate through the feed and food chain reaching 150 µg/kg in a Swiss oat bran bread (Noser et al., 2007), and mean concentrations of 47 µg/kg and 99 µg/kg, respectively, in baby foods and grain-based food products from Finnish and Italian markets, occurring in 97 % of all samples (Jestoi et al., 2004). Breakfast cereals from Tunisian and Moroccan markets contained on average 57.4 mg/kg and 10.6 mg/kg EnnB (Queslati et al., 2011; Mahnine et al., 2011). In egg yolks from laying hens fed with enniatin-contaminated feed, up to 3.8 µg/kg enniatin B was detected (Jestoi et al., 2009), demonstrating the molecule's tendency to bioaccumulate in lipophilic media.

The cyclopeptidic enniatins form ionophores with hydrophobic groups on the outside and polar groups in the core (Jestoi, 2008; Tedjiotsop Feudijo et al., 2010). They can transport mono- and divalent cations either in sandwiched complexes or by creating channels in biological membranes.

DMD Fast Forward. Published on May 26, 2011 as DOI: 10.1124/dmd.111.039529
This article has not been copyedited and formatted. The final version may differ from this version.

The primary toxic action of enniatins is thought to result from the compounds' ionophoric character. Different *in vitro* toxicity studies have elucidated their antibacterial, antihelmintic, antifungal, herbicidal and insecticidal potency (Jestoi, 2008; Tedjiotsop Feudijo et al., 2010). Enniatin B in levels up to 100 µM did not show genotoxic activity, but demonstrated cytotoxicity at low micromolar concentrations (Ivanova et al., 2006; Jestoi, 2008; Behm et al., 2009). The observed activities included e.g. the specific inhibition of acyl-coenzyme A cholesterol acyltransferase (ACAT), depolarization of mitochondria, inhibition of osteoclastic bone resorption, and induction of apoptosis in cancer cells as well as the interaction with ATP-binding cassette transporters like P-glycoprotein (Tedjiotsop Feudijo et al., 2010; Ivanova et al., 2010). The treatment of bacterial infections in the upper respiratory tract by a fusafungin-called mixture of enniatins A, A1, B, B1 in a 1% nasal inhalation solution is the only approved application in humans (Lohmann, 1988; Kroslák, 2002).

Despite the considerable range of enniatin's pharmacological and toxicological properties and the mycotoxin's prevalence in grain-based food and feed, only a few studies determining the *in vivo* potency have been conducted so far. There are no reports of natural cases of mycotoxicosis in humans or animals, but feeding experiments have shown that chronic exposition may lead to sub-acute effects like feed refusal, weight loss and reduced productivity (Jestoi, 2008). Acute toxicity and death occurred only after intraperitoneal application of 10-40 mg/kg*d body weight (BW) over six days to HIV-infected immune deficient (SCID) mice (McKee et al., 1997), whereas per oral (po) dosage of 0.5 - 1 g/kg*d BW in six days to mice and single doses of up to 50 mg/kg BW in rats did not produce toxic effects (Gäumann et al., 1950; Lohmann, 1988; Bosch et al., 1989).

The lack of correlation between *in vitro* and *in vivo* toxicity is presumably the result of low bioavailability p.o., which may be caused by impaired uptake from the gastrointestinal tract due to low compound water solubility (Blais et al 1992) and interaction with efflux

pumps (Ivanova et al, 2010), or by elimination from the systemic circulation due to metabolism reactions. However, the pharmacokinetic properties and biotransformation products of enniatins have not yet been characterized.

Considering the evaluation of enniatins as potential drug candidates and emerging toxins it was the aim of the present study to investigate the metabolism of enniatin B by performing *in vitro* elimination studies in rat, dog and human liver microsomes and cytochrome P450 reaction phenotyping with chemical inhibitors selective for human enzymes.

Materials and methods

Chemicals

EnnB was isolated and purified from rice cultures of *Fusarium avenaceum* (Ivanova et al., 2006). Nicotinamide adenine dinucleotide phosphate sodium salt (NADP), nicotinamide adenine dinucleotide phosphate reduced tetrasodium salt (NADPH), D-glucose 6-phosphate sodium salt, D-glucose 6-phosphate dehydrogenase from baker's yeast (*S. cerevisiae*), (+)-N-3-benzylnirvanol, quinidine, furafylline, sulfaphenazole and diethyldithiocarbamate were purchased from Sigma-Aldrich (St. Louis, Missouri, USA). Troleandomycin was supplied by Santa Cruz Biotechnology, Inc. (Santa Cruz, USA). Acetonitrile (Romil, Cambridge, UK or Rathburn, Walkerburn, Scotland) and dimethyl sulfoxide (DMSO; Sigma-Aldrich) were of HPLC quality or analytical-reagent grade. Formic acid (HCOOH) and ammonium formate (NH_4COO) were purchased from Merck (Darmstadt, Germany) and Sigma-Aldrich, respectively.

Microsomal Source

The metabolism and reaction phenotyping studies were performed with commercially available liver microsomes (Celsis In Vitro Technologies, Baltimore, MD, USA). Human liver microsomes (HLM) consisted of a mixed gender pool of 50 donors (No. X008067 - Lot GJA) resulting in a preparation with moderate and average CYP P450 activity suitable for stability and clearance studies. Dog liver microsomes (DLM) were prepared from male Beagle dogs (No. M00201 - Lot LNY) and rat liver microsomes (RLM) were obtained from male Wistar rats (No. M00021- Lot NYB). All microsomal preparations were stored in liquid nitrogen until use. The total CYP P450 content, protein concentrations and specific activities of the different CYP P450 isoforms were as supplied by the manufacturer.

DMD Fast Forward. Published on May 26, 2011 as DOI: 10.1124/dmd.111.039529
This article has not been copyedited and formatted. The final version may differ from this version.

LC-MS analysis of EnnB and EnnB-metabolites

EnnB and EnnB-metabolites produced by incubation with HLM, DLM, and RLM were determined by high performance liquid chromatography-coupled mass spectrometry (LC-MS) using a Finnigan Surveyor MS Pump Plus with Autosampler Plus connected via an electrospray interface to a Finnigan LTQ linear ion trap mass spectrometer (all Thermo Fisher Scientific Inc., Waltham, MA, USA). The mass analyzer was run in the full-scan mode (*m/z* 200-1000), and the electrospray interface was operated in the positive mode. The parameters of the ESI interface were adjusted as follows: a spray voltage of 4 kV, a capillary temperature of 300 °C, a tube lens offset of 100 V, a sheath gas rate of 55 L/min. and an auxiliary gas rate 5 L/min. Separation was achieved using a SunFire C_{18} column (50 × 2.1 mm; 3 µm; Waters, Milford, MA, USA) with 0.5 µm pre-column filter (Supelco, Bellefonte, PA, USA). Separation was achieved by linear gradient elution using acetonitrile (A) - water (B) (both containing 2mM NH_4COOH and 2mM HCOOH) at a flow rate of 0.35 ml/min, starting at 30% acetonitrile and rising to 100% within 8 min.

The EnnB molecule produced ion peaks at $[M+H]^+$, $[M+NH_4]^+$ and $[M+Na]^+$ with molecular ion masses of *m/z* 640, 657 and 662, respectively. $[M+NH_4]^+$ rendered the most intense and stable signal due to the high amount of ammonium salt in the mobile phase, and was therefore selected for EnnB quantitation. Additionally, the ratio of the three molecular ions was continuously monitored. EnnB was quantified comparing sample peak areas with an external calibration curve of EnnB in methanol in the concentration range 3.5 – 465.6 ng/ml. The repeatability and reproducibility of the method were evaluated by analysing replicates on different days, and accuracy was determined by recovery experiments determining EnnB spiked into the microsome assay reaction mixture.

Incubation aliquots were analysed and potential EnnB-metabolites were identified by mass and respective peak retention times relative to EnnB. Metabolite concentrations were

DMD Fast Forward. Published on May 26, 2011 as DOI: 10.1124/dmd.111.039529
This article has not been copyedited and formatted. The final version may differ from this version.

estimated by using the external EnnB-calibration curve since reference materials for the metabolites were unavailable. The structures of EnnB microsomal metabolites were tentatively identified using ion trap mass spectrometry, multiple-stage MS^n fragmentation experiments and high-resolution mass spectrometry. The instrumental analyses were supplemented with specific derivatisation reactions for tagging of functional groups. Detailed data on the structure determination of the EnnB microsomal metabolites can be found elsewhere (Ivanova et al., 2011. *In vitro* phase I metabolism of the depsipeptide enniatin B. *Anal. Bioanal. Chem*., doi 10.1007/s00216-011-4964-9).

Incubation Conditions

Substrate depletion assays monitoring the concentration-time course of EnnB were performed in RLM, DLM, and HLM under conditions of assumed first-order kinetics to determine the assay half-life ($t_{½,\ assay}$). EnnB was incubated in a reaction mixture containing NADPH-generating system (0.91 mM NADPH, 0.83 mM $NADP^+$, 19.4 mM glucose-6-phosphate, 1 U/ml glucose-6-phosphate dehydrogenase, 9 mM magnesium chloride hexahydrate), incubation buffer (45 mM Hepes pH 7.4) and 2 mg microsomal protein in a total volume of 1 ml. After preincubation at 37 °C for 3 min the reaction was initiated by adding EnnB dissolved in acetonitrile to final concentrations ranging from 0.66 µM to 1.74 µM. The fraction of acetonitrile in the microsomal incubation system was never higher than 0.3 %.

The reaction mixtures were incubated at 37 °C in a shaking waterbath (OLS 200, Grant, Cambridge, UK) in capped round-bottom glass tubes and 150 µl sample aliquots were drawn after 0, 2.5, 5, 10, 15 and 30 min and enzyme activities were stopped immediately with 150µl ice-cold acetonitrile. Samples were kept on ice until centrifugation (Eppendorf, Hamburg, Germany) at 2000 × g for 5 min to precipitate the proteins. Supernatants were collected,

DMD Fast Forward. Published on May 26, 2011 as DOI: 10.1124/dmd.111.039529
This article has not been copyedited and formatted. The final version may differ from this version.

transferred to HPLC sample vials and stored at −20 °C until LC-MS analysis. Reaction samples without the NADPH-regeneration system served as negative controls and reaction samples without EnnB were used as vehicle controls for background subtraction. All incubations were performed at least three times and in duplicate.

Formation of EnnB-metabolites

The formation of EnnB metabolites was observed in incubations with 0.66 µM in RLM, DLM, or HLM and metabolite concentration/time-curves were generated. Formation rates were calculated by determining the metabolite produced per time assuming initial reaction velocity linearity. Additionally, metabolite formation was observed in RLM with 0.88 µM and 1.74 µM EnnB initial concentrations.

Determination of Kinetic Parameters

In substrate depletion experiments, EnnB peak heights were determined and normalized to the value obtained at t = 0. The percentage remaining versus time was fitted to a first order decay function to determine the initial substrate depletion rate constant and the half-life of EnnB in the assay ($t_{1/2,assay} = \ln 2 / k$) for the different microsomal preparations. If the substrate decline showed nonlinearity in the log percentage remaining versus time curves at later incubation times, only the initial time points with apparent log-linearity were used to determine $t_{1/2,\ assay}$.

The assay clearances (CL_{assay}) were calculated from $t_{1/2,assay}$ and the assay volume (V_{assay}) according to $CL_{assay}=V_{assay} * k = V_{assay} * \ln 2 / t_{1/2,assay}$. Assuming that protein binding of EnnB in the reaction mixture was negligible (fraction unbound in the assay ($f_{u,assay} \sim 1$)), the assay clearance was an approximation of the intrinsic assay clearance ($CL_{int,assay}$), which is a measure of enzyme activity derived from the Michaelis-Menten equation parameters maximal

DMD Fast Forward. Published on May 26, 2011 as DOI: 10.1124/dmd.111.039529
This article has not been copyedited and formatted. The final version may differ from this version.

velocity ($V_{max,assay}$) and reaction constant ($K_{M,\ assay}$) under the condition that the substrate concentration in the assay is well below the K_M-value ($CL_{int,\ assay} = V_{max,assay} / K_{M,assay}$).

$K_{M,assay}$ was determined from depletion experiments with different initial EnnB concentrations by plotting the depletion rate constants to the substrate (S) concentrations. The inflection point of the curve in a lin-log plot represents the K_M value, occurring when k is half of the theoretical maximum k at infinitesimally low-substrate concentration ($k = k_{[S]\rightarrow 0} * (1 - [S]/([S]+K_M))$ (Obach and Reed-Hagen, 2002).

The respective $CL_{int,assay}$ for human, dog and rat microsomes were upscaled to the assay-independent, intrinsic liver clearances (CL_{int}) by considering the amounts of microsomal protein in the assays ($Prot_{assay}$) and the relative liver weights (RLW), and by using specific microsomal recovery indexes (MRI) (Barter et al., 2007; Smith et al., 2008) for mg of microsomal protein to g of liver ($CL_{int} = CL_{int,assay} * MRI * RLW / Prot_{assay}$).

In vitro in vivo extrapolation (IVIVE) was attempted by applying the well-stirred liver model (Obach et al., 1997; Ito and Houston, 2005). Systemic blood clearances (CL_b) were calculated from the CL_{int} by considering the hepatic blood flow (Q) of the different species ($CL_b = Q * Cl_{int} * f_{u,b} / (Q + Cl_{int} * f_{u,b})$). Since binding data for EnnB were not available, the fraction unbound ($f_{u,b}$) EnnB in blood was set to 1 for no binding.

The bioavailability (f) after p.o. application was calculated for EnnB from the CL_b ($f = f_a * (1 - CL_b / Q)$ assuming complete absorption from the gastrointestinal tract ($f_a = 1$), which allowed the estimation of the maximal bioavailability ($f_{max} = f (f_{a \rightarrow 1})$).

By inclusion of data from an older study (Lohmann, 1988) determining the *in vivo* half-life in blood ($t_{1/2,b}$) after intra-nasal (i.n.) application of tritiated EnnB to Wistar rats, the volume of distribution in blood at steady state was calculated ($V_{ss,b} = t_{1/2,b} * CL_b / ln2$) to deliver an estimate on EnnB tissue distribution.

DMD Fast Forward. Published on May 26, 2011 as DOI: 10.1124/dmd.111.039529
This article has not been copyedited and formatted. The final version may differ from this version.

Finally, the CL_b values for the three species were examined for linear correlation in the allometric scaling of clearance to body weights (BW) (log CL_b ~ log BW) (Obach et al., 1997). An average BW values of 70 kg for humans, 11 kg for Beagle dogs and 0.2 kg for Wistar rats was used in the calculations.

CYP P450 reaction phenotyping by selective human enzyme inhibitors

The effect of several specific chemical inhibitors of human CYP-enzymes on the biotransformation of EnnB was investigated in HLM. Standard assay conditions and a single concentration of EnnB (0.66 µM), lower than the estimated K_M value, were used. In this preliminary study, only one concentration close to the published optimum of effectivity and selectivity was used for each inhibitor (Pelkonen et al., 2008). CYP1A2-activity was inhibited with furafylline (Fur;10 µM), CYP2C9 with sulfaphenazole (Sul; 20 µM), CYP2C19 with N-3-Benzylnirvanol (Benz; 5µM), CYP2D6 with quinidine (Qui; 5 µM), CYP2E1 with diethyldithiocarbamate (DDC; 50 µM), and CYP3A4 was inhibited with troleandomycin (TAO; 50 µM). Additionally, Fur and TAO were used in a screening study in RLM and DLM.

All inhibitors were pre-incubated for 2 min in the presence of the NADPH-generating system and microsomes at 37 °C before the addition of EnnB. Pre-incubating for 15 min was tested for the mechanism-based inhibitors TAO and Fur showing no difference in comparison to the 2 min pre-incubation. All experiments were performed at least three times and in duplicates. A vehicle control for background subtraction, a negative control lacking the NADPH-regenerating system to exclude non-enzymatical EnnB degradation, and a toxin stability test in incubations without microsomes were additionally performed. The final solvent concentrations (DMSO; CH_3CN) in the assays were ≤ 0.3% (v/v).

The half-life of EnnB depletion was compared in the presence and absence of the chemical inhibitors, and the inhibition of EnnB depletion was estimated as a measure for the

DMD Fast Forward. Published on May 26, 2011 as DOI: 10.1124/dmd.111.039529
This article has not been copyedited and formatted. The final version may differ from this version.

interaction of EnnB with the respective CYP P450 enzymes. The magnitudes of inhibition expressed as ratios of inhibitor concentration at the active site of the cytochrome P450 enzyme ([I]) and inhibition constant (K_i) were estimated by using the percentage increase (R) in area under the concentration-time curve (AUC) in the assays in the presence and absence of the chemical inhibitors ($R = AUC_{inhib}/AUC = 1 + [I]/K_i$) or equivalently, by using the percentage increase in half-lives $R = t_{1/2,inhib} / t_{1/2} = 1 + [I]/K_i$), considering that $AUC_{assay} = Dose/CL_{assay} = [EnnB_o]*V_{assay}*t_{1/2,assay} / (ln2*V_{assay})$ resulting in $AUC \sim t_{1/2}$ (Eagerling et al., 1998; Zhang et al., 2009).

Results

Analysis of EnnB and EnnB-metabolites

The LC-MS method allowed the specific and semi-quantitative determination of EnnB (Figure 1) in sample aliquots of microsomal incubations. EnnB was determined with high precision and accuracy without interference of the microsomal matrix. The initial EnnB assay concentration (0.42 µg/µl) was in the middle of the LC-MS method's working range considering dilution in sample preparation.

EnnB-metabolites were identified by LC-retention times and specific masses obtained by high-resolution MS/MS-experiments (Ivanova et al., 2011. *In vitro* phase I metabolism of the depsipeptide enniatin B. *Anal. Bioanal. Chem.*, doi 10.1007/s00216-011-4964-9). In total, the structures of 12 main metabolites could be described (Table 1). They could be divided into three sets based on the functional groups that had been introduced into the EnnB-molecule by different biotransformation reactions: mono-oxygenated metabolites (M1 to M5), mono- and di-demethylated metabolites (M6 and M7, respectively), and di-oxygenated metabolites (M8 to M12). Considering the retention times observed by the LC-gradient, M8 to M12 were the most hydrophilic metabolites, followed by M1 to M5, and M6 and M7.

The metabolites M8 to M12 are products of sequential oxidations as indicated by their mass differences compared to EnnB. This was confirmed in an experiment by isolating M1 and M2 from RLM incubation aliquots and continued metabolisation in DLM leading to M9 to M12 (data not shown).

Metabolite formation in rat, dog and human microsomes

The concentration-time curves of EnnB-metabolite formation in RLM, DLM, and HLM showed different profiles (Figure 2). The occurrence and formation rates of the individual

metabolites differed considerably in the three microsomal preparations. M8 was only observed in trace amounts and not included into the evaluation.

In RLM, only mono-oxygenated M1 to M5 and the two demethylated species M6 and M7 were measured after 30 min incubation. The initial metabolite formation velocities (v) were highest for M6 (0.0026 µg/(ml*min)) and M2 (0.0009 µg/(ml*min)) and lowest for M4 and M7 (both 0.0002 µg/(ml*min)). M6 was the main metabolite after 30 min.

In DLM, the mono-oxygenated M1, M2 and M3 were rapidly formed (v = 0.0176 µg/(ml*min), 0.0156 µg/(ml*min), and 0.0024 µg/(ml*min), respectively), M1 showing the highest concentration after 5 min of incubation. However, concentrations declined rapidly after reaching the maximum, probably because of further oxidation to the di-oxygenated metabolites. The formation of M9, M10, M11 and M12 (v = 0.024 µg/(ml*min), 0.0004 µg/(ml*min), 0.0053 µg/(ml*min), and 0.0007 µg/(ml*min), respectively) started with a time lag of about 2.5 to 10 min after incubation start. M11 was the main biotransformation product of EnnB in DLM after 30 min. The mono-demethylated M6 (v = 0.0056 µg/(ml*min)) reached maximum concentration at 5 min; however, the di-demethylated M7 was not observed.

In HLM, the concentrations of the mono-oxygenated metabolites M1, M2, M3, and M5 increased rapidly within the first 10 min of incubation (v = 0.0026 µg/(ml*min), 0.0097 µg/(ml*min), 0.0034 µg/(ml*min), and 0.0030 µg/(ml*min), respectively). M2 was the major metabolite after 10 min, twice as high in concentration as the secondly positioned M3. The di-oxygenated metabolites M9, M11, and M12 became observable after a time lag of about 5 to 10 min. M11 was formed most rapidly (v = 0.0020 µg/(ml*min)) and was the predominant metabolite after 30 min incubation. The demethylated M6 (v = 0.0033 µg/(ml*min)) reached a concentration maximum after 15 min incubation and then decreased slowly. In contrast, M7 was not present in measurable amounts.

DMD Fast Forward. Published on May 26, 2011 as DOI: 10.1124/dmd.111.039529
This article has not been copyedited and formatted. The final version may differ from this version.

RLM assays were performed using three different EnnB initial concentrations (c) and formation velocities of the major metabolites were estimated. However, the graph v = f(c) did not seem to follow Michaelis Menten-kinetics for the respective metabolites, and therefore, formation constants (K_M) could not be determined (data not shown).

Kinetics of Enniatin B depletion

EnnB was rapidly metabolised in RLM, DLM and HLM. EnnB assay half-lifes were calculated from the initial substrate depletion rate constants of first order decay functions in the three incubation systems (Figure 3). Additionally, a direct curve fit of the non-logarithmic graphs was performed, confirming the data obtained. Under the chosen assay conditions, EnnB half-lifes in RLM, DLM, and HLM were 32 min, 4.5 min, and 12.4 min, respectively.

These data could only be used for the calculation of derived pharmacokinetic parameters if the depletion assays were performed in compliance with Michaels-Menten-kinetics requiring that the EnnB-concentration was clearly lower than the K_M-value. In view of the difficulties to obtain K_M from metabolite formation, K_M was therefore determined directly from depletion experiments in RLM with three different EnnB initial concentrations (Figure 4). The K_M was found as 1.1 µM, confirming that the initial EnnB concentration of 0.66 µM, generally used in the metabolism and inhibition assays, was well below the K_M.

Prediction of in vivo pharmacokinetic parameters

Based on the respective $t_{1/2,assay}$, the EnnB assay clearances were calculated, and applying published consensus values for *in vitro/in vivo* extrapolation, intrinsic clearances (CL_{int}) and systemic blood clearance (CL_b) were estimated using the non-restrictive well-stirred liver model (Table 2). The CL_b were 1.57 l/(h*kg) in rats, 1.67 l/(h*kg) in dogs, and 0.63 l/(h*kg) in humans leading to predicted maximal bioavailabilities of 63 %, 20 %, and 55% under the

assumption that EnnB is completely absorbed from the gastro-intestinal tract after oral application, which is truly a considerable overestimation.

According to an older study applying fusafungin-carried tritiated EnnB in a total dosage of 10 mg/kg in isotonic saline to Wistar rats (Lohmann, 1988), the ratio between renally and fecally excreted radioactivities was approximately 1:12. Roughly, the fraction absorbed could be estimated as $f_a = 0.08$, under the condition that the administered compound was solved in the saline formulation. Applying f_a for the prediction of EnnB bioavailability in rats using the data from the microsomal assay resulted in $f = f_{max} * f_a = 5$ %, which was the same value as found in the cited study for the amount of renally excreted total radioactivity.

Protein binding in the microsomal assays ($f_{u,assay}$) and in blood ($f_{u,b}$) were ignored in the present approach to predict *in vivo* pharmacokinetic parameters of EnnB. In the equation for the well-stirred liver model, drug binding to microsomes and blood would cancel out if the unbound fraction is the same in both matrices (Ito and Houston, 2005).

An estimate for the volume of distribution in blood at steady state ($V_{ss,b}$) in rats was calculated from the blood clearance ($CL_b = 1.57$ l/(h*kg)) that was predicted in the present study, and a value for the maximal half-life in blood ($t_{1/2,b} = 0.5$ h) derived from the measurement of total radioactivity decline in blood after intra-nasal application of tritiated EnnB (Lohmann, 1988). Comparison of the value determined ($V_{ss,b} = 1.13$ l/kg) with the blood volume in rats ($V_b = 0.06$ l/kg) indicates that EnnB distributes into body tissues.

The predicted CL_b of rat, dog and humans were combined to perform interspecies scaling (Figure 5) with the intention to check the probability of the determined values. Linear regression of the log/log-graph of $CL_b = f(BW)$ rendered a regression coefficient near unity ($r^2 = 0.98$), confirming that the predicted CL_b values for the three species are correlated in accordance with the principles of allometric scaling.

DMD Fast Forward. Published on May 26, 2011 as DOI: 10.1124/dmd.111.039529
This article has not been copyedited and formatted. The final version may differ from this version.

Inhibition of Enniatin B depletion by selective inhibitors of human CYP-enzymes

The *in vitro* determination of biotransformation pathways by CYP P450 reaction phenotyping is a central element in the assessment of a compound's inhibition and induction potential. In guidance documents of drug administration authorities, CYP1A2, CYP2C9, CYP2C19, CYP2D6, CYP2E1 and CYP3A4 are named as the critical enzymes for humans (Tucker et al. 2001). In the present study, the inhibitory potential of selective chemical inhibitors on the EnnB depletion in HLM was determined. Half-lifes in the presence and absence of the inhibitors were determined and used to calculate ratios of inhibitor concentration to inhibition constant ([I]/K_i-values) for each inhibitor/EnnB combination.

The CYP-enzyme phenotyping in HLM showed that the most effective inhibition of EnnB-biotransformation was achieved by blocking CYP3A4, CYP2C19 and CYP2A1 (Figure 6). Comparing EnnB concentrations after 30 min incubation with and without selective inhibitors, respectively 62 %, 51 %, and 54 % inhibition were observed. In contrast, the inhibition of CYP2E1, CYP2C9 and CYP2D6 had less effect on EnnB metabolism, showing respectively 35 %, 9%, and 3% inhibition effectivity. The calculated [I]/K_i-values reflected the probabilities of EnnB being a substrate of the individual human CYP-enzymes (Table 3). The [I]/K_i-value for EnnB's interaction with CYP3A was about eight times higher than for CYP1A2, CYP2C19 and CYP2E1, which still could considerably contribute to the EnnB metabolism. In contrast, the involvement of CYP2C9 and CYP2D6 was less probable.

Additionally, the mechanism-based inhibitors Fur and TAO were used in a screening study in RLM and DLM showing that the inhibition potencies for EnnB biotransformation were comparable in HLM and DLM, and lower in RLM. In both animal species, enzymes belonging to the CYP1A and CYP3A families could be involved in EnnB metabolism (Figure 6). The provisional [I]/K_i-values, which were generated in an attempt to describe the observations (Table 3), supported the findings.

DMD Fast Forward. Published on May 26, 2011 as DOI: 10.1124/dmd.111.039529
This article has not been copyedited and formatted. The final version may differ from this version.

Discussion

Enniatins have been called emerging mycotoxins (Jestoi, 2008; Tedjiotsop Feudijo et al., 2010) showing cellular toxicity at low micromolar concentrations (Ivanova et al., 2006; Firkova et al., 2007). The extensive low-level exposure of humans and animals to enniatins in food and feed has led to increased awareness of the responsible food authorities. The European Food Safety Agency (EFSA) has issued in 2010 a call for enniatin occurrence data (http://www.efsa.europa.eu/en/datexdata/docs/InstructionMycoPhytotoxins.pdf) with the aim to prepare a scientific opinion on the risk to human and animal health.

While reports on acute mycotoxicosis for enniatins are lacking, there is concern with regard to sub-acute toxicity. *In vivo* toxicity data are sparse, and the few data available reveal a missing correlation to *in vitro* toxicity studies. A PhD-thesis dealing with "analytical, pharmacological and microbiological investigations of the ionophoric antibiotic fusafungin" (Lohmann, 1988) included *in vivo* experiments applying tritiated EnnB p.o and i.n. to rats, and revealed the compound's relatively low bioavailability and short half-life. Furthermore, it was shown by *in vitro* incubations with rat liver cytosol that EnnB was not a substrate for phase II-metabolism.

The study presented here used an *in vitro* approach with liver microsomes from different species for the identification of EnnB's biotransformation products by phase I-metabolism and the prediction of pharmacokinetic parameters. *In vitro* metabolic systems have successfully been employed to study drug metabolism, kinetics and CYP P450 enzyme inhibition and models and procedures for the prediction of *in vivo* data from *in vitro* metabolism data have been developed (Iwatsubo et al., 1997; Obach et al., 1997; Naritomi et al., 2001; Riley et al., 2005; Ito and Houston, 2005; De Buck et al., 2007).

EnnB was metabolised by rat, dog and human microsomes, and produced metabolites were analyzed by LC-MS. The method used allowed the quantitative determination of EnnB

concentrations in incubation aliquots and the identification and semi-quantitation of the EnnB-metabolites (Ivanova et al., 2011. *Anal. Bioanal. Chem.*, doi 10.1007/s00216-011-4964-9). The 12 characterized metabolites were products of oxidative reactions (Guengerich, 2001) including carbon hydroxylation (M1, M2, M3, M4), N-methyl-oxydation (M5), dealkylation (M6, M7), carbon hydroxylation and aldehydation (M8), and carbon hydroxylation and carboxylation (M9, M10, M11, M12). Consequently, the EnnB-metabolites were more hydrophilic than their parent compound, which was confirmed by the respective retention times in reversed-phase chromatography.

The characterization of metabolites is an important step in the safety and risk evaluation of a compound. Reactive metabolites can affect the overall toxic profile and have to be assessed with regard to exposure, half-live, matrix of occurrence, and toxicity mechanism (Smith and Obach, 2009). EnnB metabolite formation data obtained in the present study showed slower rates and a different profile for rats compared to dogs and humans. Demethylation was favoured over hydroxylation, and products of multiple oxidation reactions were not observed, which dominated in dogs and humans. This implied that different P450 enzymes are involved in the EnnB biotransformation in the three species. Furthermore, the occurrence of isobaric metabolites suggested multiple reaction points for the metabolizing enzymes in the EnnB-molecule. K_M for metabolite formation could not be determined on the basis of three EnnB concentrations, either because metabolite concentrations were measured incorrectly due to the lack of metabolite reference materials or because concentrations were too high compared to the respective K_M. Therefore, metabolite kinetics should be examined further in a follow-up study.

EnnB depletion kinetics revealed dissimilar assay half-lifes in RLM, DLM, and HLM mirroring the differences in metabolite formation. The depletion K_M (Obach and Reed-Hagen, 2002) was determined for rats as the slowest EnnB-metabolizer confirming that the initial

DMD Fast Forward. Published on May 26, 2011 as DOI: 10.1124/dmd.111.039529
This article has not been copyedited and formatted. The final version may differ from this version.

EnnB concentration of 0.66 µM used in all subsequent assays was sufficiently low to allow reactions to run under first-order kinetics. The advantage of determining K_M directly from EnnB-half lifes in preference to using metabolite formation rates is that authentic metabolite standards are unnecessary. The approach has been proven to comply with drug screening purposes.

The IVIVE calculations were performed using published consensus factors for MRI, RLW, and Q (Iwatsubo et al., 1997; Barter et al., 2007; Smith et al., 2008) in the non-restrictive well-stirred liver model (Naritomi et al., 2001; Riley et al., 2005).The results indicated that EnnB is a intermediate to high-clearance drug. Although EnnB is considerably lipophilic and tends to bioaccumulate (Jestoi et al., 2009), binding to microsomes ($f_{u,assay}$) and binding to plasma proteins ($f_{u,b}$) was disregarded in the predictions assuming that they were similar and the unbound fraction terms would therefore cancel out from the equations (Obach et al., 1997; Ito and Houston, 2005). This strategy has been shown to work most successfully in several extensive drug metabolism studies yielding the best agreement (85 %) between observed and predicted CL_b-values (De Buck et al., 2007; Wan et al., 2010).

Probabilistic proof of the obtained results by means of allometric scaling was reassuring as it confirmed species interrelation with regard to clearance and body weight in accordance to the empirically found principle (Obach et al., 1997; Ito and Houston, 2005). Furthermore, when data obtained from a metabolism experiment with primary rat hepatocytes were included into the calculation base, the regression coefficient dropped only with 0.01 (data not shown) confirming previous results (Lohman, 1988) that conjugative phase II-metabolism is most likely irrelevant for EnnB.

Data from a prior p.o rat study with application of tritiated EnnB allowed the approximation of additional pharmacokinetic parameters such as f_a and $t_{1/2}$ (Lohmann, 1988). However, the ^{3}H-label had been incorporated into the methyl group of the EnnB molecule's

DMD Fast Forward. Published on May 26, 2011 as DOI: 10.1124/dmd.111.039529
This article has not been copyedited and formatted. The final version may differ from this version.

N-Me-Val moiety, which is subject to heteroatom oxygenation (M5) and dealkylation (M6, M7) reactions, potentially leading to the loss of the label. Therefore, the total amount of EnnB and EnnB-metabolites may have been underestimated by determining total radioactivity. In consequence, the estimates for f_a and $t_{1/2}$ might be too low.

Nevertheless, some valuable information could be drawn by combining the *in vivo* data with the rat CL_b-value obtained by the present study. The bioavailability of EnnB was predicted to be low and the distribution into body tissues to be of considerable size, providing an explanation for the absence of acute toxicity and suspected sub-acute effectivity. Bioaccumulation in liver, kidney and brain had also been found in the study with ^{3}H-EnnB.

A preliminary risk assessment was attempted by calculating EnnB exposure on the basis of the available *in vivo* rat data and the predicted rat and human clearances. The maximum concentration in blood ($C_{max,b}$) was reached in rats after 30 min (t_{max}). Assuming that the ratio of volume of distribution to blood volume is comparable in humans and rats ($V_{b,\ human}$ = 0.07 l/kg; $V_{ss,b\ human}$ = 1.35 l/kg) and using maximum values of food contamination ([EnnB]) and large-scale consume (A) to calculate a dose (dose = [EnnB] * A), a theoretical $C_{max,b}$ was determined ($C_{max,b} = f_{max,human} * f_{a,rat} * dose * e^{(-ln2*tmax/t1/2)} / * V_{ss,b}$) for adults (70 kg) and compared to IC_{50} in *in vitro* cytotoxicity assays. The consumption of e.g. 500 g Swiss oat bread (Noser et al., 2007) would lead to $C_{max,b}$ = 0.03 µM, delivering a safety factor of about 100. However, by eating 300 g of Tunisian breakfast cereals (Queslati et al., 2011) $C_{max,b}$ = 6.3 µM would be reached, which is a level of concern.

The CYP-enzyme phenotyping experiments in this study showed that human CYP3A4, CYP2C19 and CYP1A2 likely played major roles in EnnB biotransformation. EnnB's susceptibility to CYP3A4 metabolism and transport by P-glycoprotein (Ivanova et al. 2010) are possibly responsible for the compound's low absorption rate (f_a) considering the substantial CYP3A4-activity in the gastrointestinal tract.

DMD Fast Forward. Published on May 26, 2011 as DOI: 10.1124/dmd.111.039529
This article has not been copyedited and formatted. The final version may differ from this version.

The catalytic selectivity of CYP P450 subfamily enzymes from different species can vary considerably (Bogaards et al., 2002), but selective inhibitors of human CYP-enzymes have also been used for reaction phenotyping in other species (Eagling et al., 1998; Martignoni et al., 2006). The mechanism-based inhibitors Fur and TAO have been successfully used for cross-species evaluations of CYP1A and CYP3A-catalyzed biotransformations, respectively (Chauret et al., 1997; Quinteri et al., 2008; Aueviriyavit et al., 2010). Qualitatively similar results were obtained in human and animal microsomes although the enzyme reaction rates differed (Quinteri et al., 2008), which was ascribed differences in the formation of the metabolic intermediate complexes (Aueviriyavit et al., 2010).By comparing the percentage increase in $t_{1/2}$ with and without inhibitors, we have attempted to show the relative magnitudes of inhibition potentials. The derived [I]/K_i-values describe a compound's inhibitory potential on CYP P450 model substrates (Zhang et al., 2009); however, in the present study, the approach was modified in estimating to which extent EnnB-biotransformation could be expected to take course via the different pathways (Pelkonen et al., 2008).

The EnnB-depletion inhibition is equivalent to the decrease in intrinsic enzyme clearances, independently from the mechanism of inhibition. The inhibition of EnnB-metabolite formation, the determination of K_i-values, and correlation of metabolite structures to the respective P450-enzyme reactions could be characterized in a subsequent study. Furthermore, the inhibitor potential of EnnB could be assessed using isoforms-specific substrate probes.

Authorship Contributions

Participated in research design: Ivanova, and Fæste

Conducted experiments: Ivanova

Contributed new reagents or analytical tools: Ivanova, and Uhlig

Performed data analysis: Fæste, Ivanova, and Uhlig

Wrote or contributed to writing of the manuscript: Fæste, Ivanova, and Uhlig

References

Altomare C, Logrieco A, Bottalico A, Mulé G, Moretti A, and Evidente A (1995). Production of type A trichothecenes and enniatin B *Fusarium sambucinum* Fuckel sensu lato. *Mycopathologia* **129**:177-181.

Aueviriyavit S, Kobayashi K, Chiba K (2010). Species differences in mechanism-based inactivation of CYP3A in humans, rats and mice. *Drug Metab Pharmacokinet.* **25**:93-100.

Barter ZE, Bayliss MK, Beaune PH, Boobis AR, Carlile DJ, Edwards RJ, Houston JB, Lake BG, Lipscomb JC, Pelkonen OR, Tucker GT, and Rostami-Hodjegan A (2007). Scaling factors for the extrapolation of in vivo metabolic drug clearance from in vitro data: reaching a consensus on values of human microsomal protein and hepatocellularity per gram of liver. *Curr Drug Metab* **8**:33-45.

Behm C, Degen GH, and Follmann W (2009). The *Fusarium* toxin enniatin B exerts no genotoxic activity, but pronounced cytotoxicity *in vitro*. *Mol Nutr Food Res* **53**:423-430.

Blais LA, Apsimon JW, Blackwell BA, Greenhalgh R, and Miller JD (1992). Isolation and characterization of enniatins from fusarium-avenaceum Daom-196490. *Can J Chem* **70**:1281-1287.

Bogaards JJ, Bertrand M, Jackson P, Oudshoorn MJ, Weaver RJ, van Bladeren PJ, Walther B (2000). Determining the best animal model for human cytochrome P450 activities: a comparison of mouse, rat, rabbit, dog, micropig, monkey and man. Xenobiotica 30:1131-1152.

Bosch U, Mirocha CJ, Abbas HK, and Di Menna M (1989). Toxicity and toxin production by *Fusarium* isolates from New Zealand. *Mycopathologia* **108**:73-79.

Chauret N, Gauthier A, Martin J, Nicoll-Griffith DA (1997). In vitro comparison of cytochrome P450-mediated metabolic activities in human, dog, cat, and horse. *Drug Metab Dispos*. **25**:1130-6.

De Buck SS, Sinha VK, Fenu LA, Gilissen RA, Mackie CE, and Nijsen MJ (2007). The prediction of drug metabolism, tissue distribution, and bioavailability of 50 structurally diverse compounds in rat using mechanism-based absorption, distribution, and metabolism prediction tools. *Drug Metab Dispos* **35**:649-659.

Eagling VA, Tjia JF, and Back DJ (1998). Differential selectivity of cytochrome P450 inhibitors against probe substrates in human and rat liver microsomes. *Br J Clin Pharmacol* **45**:107-114.

Firáková S, Proska B, and Šturdíková M (2007). Biosynthesis and biological activities of enniatins. *Pharmazie* **62**:563-568.

Gäumann E, Naef-Roth S, and Ettlinger L (1950). Zur Gewinnung von Enniatinen aus dem Myzel verschiedener Fusarien. *Phytopathol Z* **16**:244–289.

Guengerich FP (2001). Common and uncommon cytochrome P450 reactions related to metabolism and chemical toxicity. *Chem Res Toxicol* **14**:611-650.

Ito K, and Houston B (2005). Prediction of human drug clearance from in vitro and preclinical data using physiologically based and empirical approaches. *Pharmaceut Res* **22**:103-112.

Ivanova L, Skjerve E, Eriksen GS, and Uhlig S (2006). Cytotoxicity of enniatins A, A1, B, B1, B2 and B3 from *Fusarium avenaceum*. *Toxicon* **47**:868-876.

Ivanova L, Uhlig S, Eriksen GS, and Johannessen LE (2010). Enniatin B1 is a substrate of intestinal P-glycoprotein, multidrug resistance-associated protein 2 and breast cancer resistance protein. *World Mycotoxin J* **3**:271-281.

Iwatsubo T, Hirota N, Ooie T, Suzuki H, Shimada N, Chiba K, Ishizaki T, Green CE, Tyson CA, and Sugiyama Y (1997). Prediction of in vivo drug metabolism in the human liver from in vitro metabolism data. *Pharmacol Ther* **73**:147-71.

Jestoi M (2008). Emerging fusarium mycotoxins fusaprofilin, beauvericin, enniatins, and moniliformin – a review. *Crit Rev Food Sci Nutr* **48**:21-49.

Jestoi M, Carmela SM, Merja K, PirjoV, Aldo R, Alberto R, and Kimmo P (2004). Levels of mycotoxins and sample cytotoxicity of selected organic and conventional grain-based products purchased from Finnish and Italian markets. *Mol Nutr Food Res* **48**:299-307.

Jestoi M, Rokka M, Järvenpää E, Peltonen K (2009). Determination of *Fusarium* mycotoxins beauvericin and enniatins (A, A1, B, B1) in eggs of laying hens using liquid chromatography-tandem mass spectrometry (LC-MS/MS). *Food Chem* **115**:1120-1127.

Kroslák M (2002). Efficacy, and acceptability of fusafungine, a local treatment for both nose and throat infections, in adult patients with upper respiratory tract infections. *Curr Med Res Opin* **18**:194-200.

Lohmann A (1988). Analytische, pharmakologische und mikrobiologische Untersuchungen des ionophoren Antibiotikums Fusafungin. PhD thesis, Westfälische Wilhelms Universität, Münster, Germany.

Mahnine N, Meca G, Elabidi A, Fekhaoui M, Saoiabi A, Font G, Mañes J, and Zinedine A (2011). Further data on the levels of emerging Fusarium mycotoxins enniatins (A, A1, B, B1), beauvericin and fusaproliferin in breakfast and infant cereals from Morocco. *Food Chem* **124**: 481-485.

Martignoni M, Groothuis GM, de Kanter R (2006). Species differences between mouse, rat, dog, monkey and human CYP-mediated drug metabolism, inhibition and induction. Expert Opin Drug Metab Toxicol. 2:875-894.

McKee TC, Bokesch HR, McCormick JL, Rashid MA, Spielvogel D, Gustafson KR, Alavanja MM, Cardelline JH, and Boyd MR (1997). Isolation and characterization of new anti-HIV and cytotoxic leads from plants, marine, and microbial organisms. *J Nat Prod* **60**:431-438.

Naritomi Y, Terashita S, Kimura S, Suzuki A, Kagayama A, and Sugiyama Y (2001). Prediction of human hepatic clearance from in vivo animal experiments and in vitro metabolic studies with liver microsomes from animals and humans. *Drug Metab Dispos* **29**:1316-1324.

Noser J, Schmutz HR, Schmid S, and Schneider P (2007). Bestimmung von Enniatinen in Getreideprodukten aus dem Schweizer Markt. *Lebensmittelchemie* **61**:49-72.

Obach RS, Baxter JG, Listin TE, Silber BM, Jones BC, MacIntyre F, Ranve DJ, and Wastall p (1997). The prediction of human pharmacokinetic parameters from preclinical and in vitro metabolism data. *J Pharmacol Exp Ther* **283**:46-58.

Obach RS, and Reed-Hagen AE (2002). Measurement of Michaelis constant for cytochrome P450-mediated biotransformation reactions using a substrate depletion approach. *Drug Metab Dispos* **30**:831-837.

Pelkonen O, Turpeinen M, Hakkola J, Hankakoski P, Hukkanen J, and Raunio H (2008). Inhibition and induction of human cytochrome P450 enzymes: current status. *Arch Toxicol* **82**:667-715.

Queslati S, Meca G, Milliki A, Ghorbel A, and Mañes J (2011). Determination of Fusarium mycotoxins enniatins, beauvericin and fusaproliferin in cereals and derived products from Tunisia. Food Control, doi: 10.1016/j.foodcont.2011.02.015.

Quintieri L, Fantin M, Palatini P, De Martin S, Rosato A, Caruso M, Geroni C, Floreani M (2008). *In vitro* hepatic conversion of the anticancer agent nemorubicin to its active metabolite PNU-159682 in mice, rats and dogs: a comparison with human liver microsomes. *Biochem Pharmacol.* **76**:784-95.

Riley RJ, McGinnity DF, and Austin RP (2005). A unified model for predicting human hepatic, metabolic clearance from in vitro intrinsic clearance data in hepatocytes and microsomes. *Drug Metab Dispos* **33**:1304-1311.

Smith R, Jones RDO, Ballard PG, and Griffiths HH (2008). Determination of microsome and hepatocyte scaling factors for in vitro/in vivo extrapolation in the rat and dog. *Xenobiotica* **38**:1386-1398.

Smith DA, and Obach RS (2009). Metabolites in safety testing (MIST): considerations of mechanisms of toxicity with dose, abundance, and duration of treatment. *Chem Res Toxicol* **22**:267-279.

Tedjiotsop Feudijo F, Dornetshuber R, Lemmens M, Hoffmann O, Lemmens-Gruber R, and Berger W (2010). Beauvericin and enniatin: emerging toxins and/or remedies? *World Mycotoxin J* **3**:415-430.

Tucker GT, Houston JB, and Huang S-M (2001). Optimizing drug development: strategies to assess drug metabolism/transporter interaction potential – toward a consensus. Pharmaceut Res **18**:1071-1080.

Uhlig S, Jestoi M, and Parikka P (2007). *Fusarium avenaceum* – The North European situation. *Int J Food Microbiol* **119**:17-24.

Wan H, Bold P, Larsson LO, Ulander J, Peters S, Löfberg B, Ungell AL, Någård M, and Llinàs A (2010). Impact of input parameters on the prediction of hepatic plasma clearance using the well-stirred model. *Curr Drug Metab* **11**:583-594.

Zhang L, Zhang YD, Zhao P, and Huang S-M (2009). Predicting drug-drug interactions: an FDA perspective. AASP J **11**:300-306.

Footnotes

This work was supported in part by the Norwegian Research Council [grant nr. 200349/I10] with in the project “Mycotoxin 2 – biomarkers for adverse endocrine effects of fungal extrolites and mycotoxins – characterisation of molecular mechanisms using cell assays, chemical analyses and proteomics”.

Legends for Figures

Figure 1: Molecular structure of Enniatin B.

Figure 2: Formation of main EnnB metabolites in RLM, DLM, and HLM.

Figure 3: Enniatin B depletion in RLM, DLM, and HLM

Figure 4: K_M of EnnB depletion in RLM

Figure 5: Interspecies scaling of predicted EnnB blood clearances.

Figure 6: Inhibition of EnnB depletion by selective inhibitors of human CYP-enzymes.

DMD Fast Forward. Published on May 26, 2011 as DOI: 10.1124/dmd.111.039529
This article has not been copyedited and formatted. The final version may differ from this version.

Tables

Table 1

Main EnnB metabolites obtained in incubations with RLM, DLM, and HLM.

Metabolite	Formula[a]	Observed mass $[M+NH_4]^+$
M1 a,b	$C_{33}H_{57}N_3O_{10}$	673.4373
M2 a,b	$C_{33}H_{57}N_3O_{10}$	673.4377
M3	$C_{33}H_{57}N_3O_{10}$	673.4364
M4	$C_{33}H_{57}N_3O_{10}$	673.4377
M5	$C_{33}H_{57}N_3O_{10}$	673.4369
M6	$C_{32}H_{55}N_3O_9$	643.4265
M7	$C_{31}H_{53}N_3O_9$	629.4120
M8	$C_{33}H_{55}N_3O_{11}$	687.4164
M9	$C_{33}H_{55}N_3O_{11}$	687.4160
M10	$C_{33}H_{55}N_3O_{11}$	687.4149
M11	$C_{33}H_{55}N_3O_{11}$	687.4157
M12	$C_{33}H_{55}N_3O_{11}$	687.4161

[a]The molecular formula of enniatin B is $C_{33}H_{57}N_3O_9$

DMD Fast Forward. Published on May 26, 2011 as DOI: 10.1124/dmd.111.039529
This article has not been copyedited and formatted. The final version may differ from this version.

Table 2

Estimated kinetic parameters of EnnB, derived from *in vitro* metabolism

Parameter	RLM[a]	DLM[b]	HLM[c]
k [min^{-1}][*]	0.021	0.156	0.056
$t_{1/2,assay}$ [min]	32	4.5	12.4
$K_{M,assay}$ [µM][**]	1.1	-	-
$Cl_{int,assay}$ [l/h]	$1.28*10^{-3}$	$9.36*10^{-3}$	$3.36*10^{-3}$
Cl_{int} [l/(h*kg)]	1.16	8.23	1.13
Cl_b [l/(h*kg)]	1.57	1.67	0.63
f_{max} [%]	63	20	55
$t_{1/2,b}$ [h][***]	0.5	-	-
$V_{ss,b}$ [l/kg] [***]	1.13	-	-

[a]MRI = 61 mg/g; RLW = 40 g/kg ; $Prot_{assay}$ = 2 mg ; Q_{rat} = 4.2 l/(h*kg)
[b]MRI = 55 mg/g; RLW = 32 g/kg ; $Prot_{assay}$ = 2 mg ; Q_{dog} = 2.1 l/(h*kg)
[c]MRI = 32 mg/g; RLW = 21 g/kg ; $Prot_{assay}$ = 2mg ; Q_{human}= 1.4 l/(h*kg)
[*]determined by regression of EnnB depletion plot (Figure 2)
[**]derived from EnnB depletion (Figure 3)
[***]derived under inclusion of data from published *in vivo* study (Lohmann, 1988)

DMD Fast Forward. Published on May 26, 2011 as DOI: 10.1124/dmd.111.039529
This article has not been copyedited and formatted. The final version may differ from this version.

Table 3

EnnB[*] depletion half-lifes ($t_{1/2}$ [min]) in the absence and presence of selective inhibitors of human CYP-enzymes and [I]/K_i values[**].

	no	Fur (CYP1A2)[#]	Sul (CYP2C9)[#]	Benz (CYP2C19)[#]	Qui (CYP2D6)[#]	DDC (CYP2E1)[#]	TAO (CYP3A4)[#]
human							
$t_{1/2}$	12.	54	15.9	48	15.6	34	365
[I]/K_i	4	3.35	0.28	2.87	0.26	1.74	28.4
rat[¤]							
$t_{1/2}$	32	57	-	-	-	-	70
[I]/K_i		0.78	-	-	-	-	1.18
dog[¤]							
$t_{1/2}$	4.5	20	-	-	-	-	83
[I]/K_i		3.44	-	-	-	-	17.4

[#]human CYP P450 enzymes selectively inhibited by the respective chemical inhibitors
[¤]animal data are approximate since selective inhibitors of human CYP-enzymes were used
[*]EnnB initial concentration in all assays was 0.66 µM.
[**] Prediction of CYP interaction according to [I]/K_i values: remote, possible, likely

Figure 1

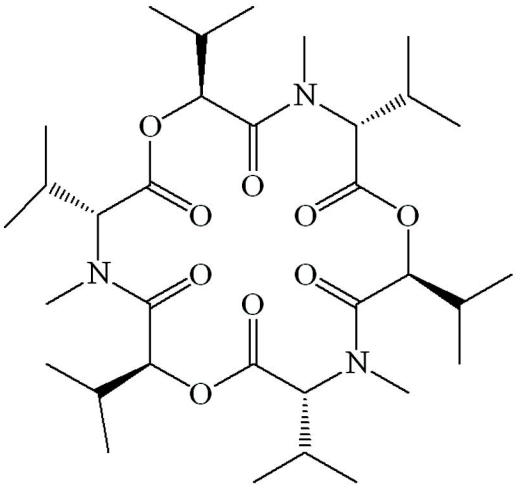

Figure 2

DMD Fast Forward. Published on May 26, 2011 as DOI: 10.1124/dmd.111.039529
This article has not been copyedited and formatted. The final version may differ from this version

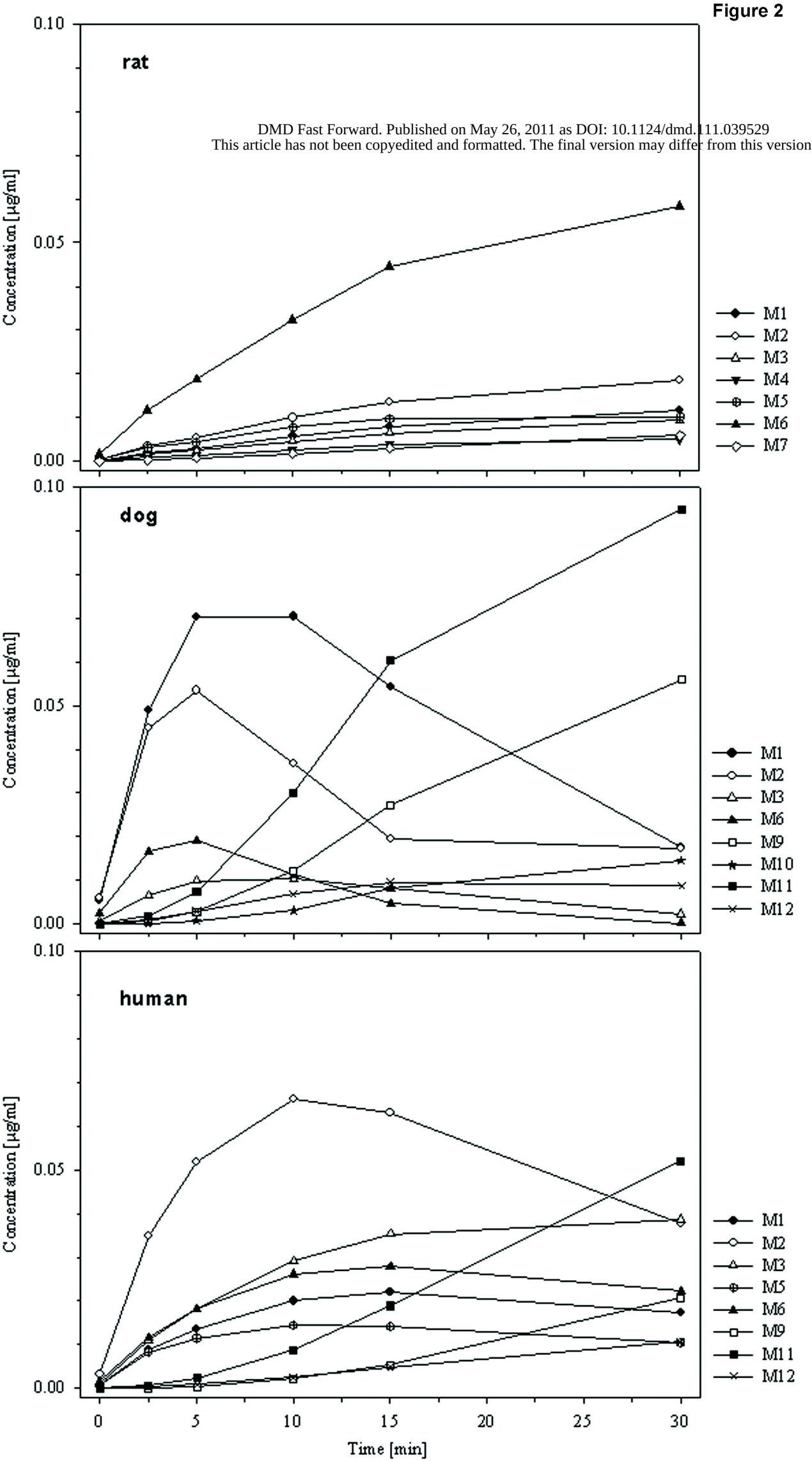

Figure 3

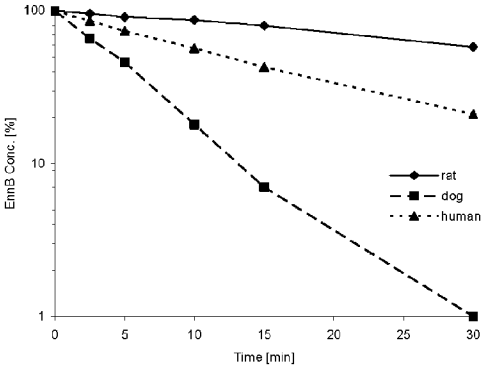

rat: y – 107.71*$e^{-0.021x}$; R^2–0. 0.9979; 3 points

dog: y = 92.82*$e^{-0.1556x}$; R^2=0.9931; 5 points

human: y = 99.082 * $e^{-0.0561*x}$; R^2=0.9992; 4 points

Figure 4

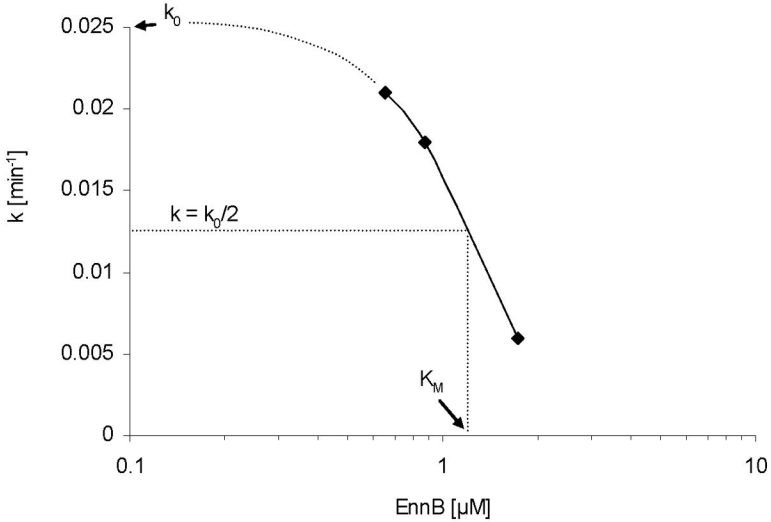

Figure 5

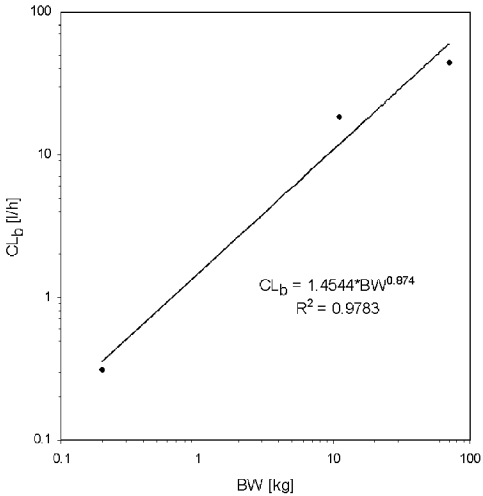

Figure 6